Computers & Geosciences 30 (2004) 1069–1077

COMPUTERS & GEOSCIENCES

www.elsevier.com/locate/cageo

DETACH: an Excel spreadsheet to simulate 2-D cross sections of detachment folds ☆

M. Scott Wilkerson[a,*], Joshua M. Wilson[a], Josep Poblet[b], Mark P. Fischer[c]

[a]Department of Geosciences, DePauw University, 602 South College Ave., Greencastle, IN 46135, USA
[b]Departamento de Geologia, Universidad de Oviedo, C/Arias de Velasco s/n, 33005 Oviedo, Spain
[c]Department of Geology & Env Geosciences, Northern Illinois University, DeKalb, IL 60115, USA

Received 17 September 2003; received in revised form 23 July 2004; accepted 10 August 2004

Abstract

Structural geologists now recognize detachment folds as fundamental structural features in many contractional settings. Several two-dimensional geometric and kinematic models exist to describe the development of such detachment folds; however, most are not available in a computer-based format that permits the forward-modeling and graphical representation of the detachment fold geometry. We developed DETACH, a Microsoft Excel™ spreadsheet, to construct simple cross sections of detachment folds using published geometric and kinematic models. DETACH allows users to assess the range of possible fold geometries and detachment depths that can be constructed using a prescribed set of fold kinematics, and to quickly evaluate and select a best-fit kinematic model for folds of known geometry. We illustrate DETACH's capabilities by modeling a two-dimensional cross section of a natural detachment fold and by constructing pseudo-three-dimensional models of detachment fold terminations with the assistance of Geosec2D™ and Gocad™ structural modeling software.

Keywords: Structural geology; Fold-thrust belt; Fault-related fold; Forward modeling; Balanced cross section

1. Introduction

Structural geologists long have recognized the significance of fault-related folds in the development of various contractional terranes, including foreland fold-thrust belts, accretionary prisms, and toe structures of extensional collapse features (e.g., Dahlstrom, 1970; Suppe, 1983; Jamison, 1987; Mitra, 1990, 1992; Suppe and Medwedeff, 1990; Wilkerson and Wellman, 1993; Apotria and Wilkerson, 2002). Detachment folds, however, have not received as much attention as other types of fault-related folds until relatively recently, as geologists began to recognize their importance and abundance (e.g., Jamison, 1987; Mitchell and Woodward, 1988; Dahlstrom, 1990; Epard and Groshong, 1993, 1995; Groshong and Epard, 1994; Hardy and Poblet, 1994; Homza and Wallace, 1995, 1997; Poblet and Hardy, 1995; Poblet and McClay, 1996; Atkinson and Wallace, 2003). Detachment folds commonly develop to accommodate shortening and displacement of rocks with different mechanical properties above (or below) a sub-horizontal slip surface or detachment (Fig. 1). Unlike other types of fault-related folds,

☆Code available at http://www.iamg.org/CGEditor/index.htm or http://www.depauw.edu/acad/geosciences/mswilke/research.asp

*Corresponding author. Tel.: +1 765 658 4666; fax: +1 765 658 4732.
E-mail address: mswilke@depauw.edu (M.S. Wilkerson).

0098-3004/$ - see front matter
doi:10.1016/j.cageo.2004.08.003

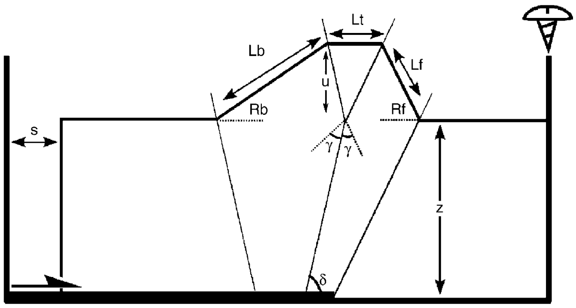

Fig. 1. Idealized detachment fold with key model parameters labeled. Layer represents interface between competent (above) and incompetent units (below). Symbols are as follows: z = detachment depth; s = shortening; Rb, Rf = backlimb and forelimb dips, respectively; Lb, Lf = backlimb and forelimb lengths, respectively; Lt = crest length; u = uplift, γ = half interlimb angle; and δ = angle between axial surface and detachment.

detachment folds form without the presence of a fault ramp and usually involve deformation of an incompetent unit immediately above the detachment. Typically, detachment folding is manifested by symmetric or asymmetric box folds with the fold cores filled by the incompetent unit.

Several geometric and kinematic models have been proposed to describe the development of detachment folds (e.g., Dahlstrom, 1990; Homza and Wallace, 1995, 1997; Poblet and McClay, 1996; Atkinson and Wallace, 2003). Most models create area-balanced detachment folds (cf. Chamberlin, 1910) by prescribing geometric relationships between shortening, detachment depth, limb dips, and limb lengths due to the kinematic processes of hinge migration, limb rotation, or a combination of the two. These models, however, often are not easily applied because (1) models must either be generated by hand or created using specialized, platform-specific software such as AutoCAD™, and (2) there are numerous variables that must be changed in order to evaluate their influence on the resultant fold geometry.

To address these issues, we developed DETACH, a Microsoft Excel™ spreadsheet that rapidly constructs simple cross sections of detachment folds. DETACH builds cross sections using geometric relations and kinematic models described by Poblet and McClay (1996). Rapid section construction allows users to easily find best-fit kinematic models for folds of known geometry, or to assess the range of fold geometries that can be created using a given set of fold kinematics. For the latter case, DETACH specifically helps constrain the detachment depth, which often is the most difficult aspect of natural detachment folds to constrain. Changes in detachment depth reflect both changes in the thickness of the incompetent unit (most commonly related to the growth and tightening of the detachment fold) and/or changes in the detachment level that might occur due to lithologic or mechanical variations within the unit hosting the detachment. Because detachment folds occur in complex contractional settings commonly associated with hydrocarbon accumulations, understanding the development and geometric characteristics of detachment folds may better facilitate the discovery and extraction of natural resources from these regions.

2. Model descriptions

Poblet and McClay (1996) provided a detailed description of the four detachment fold models programmed in DETACH. Each model consists of a single homogeneous competent unit that is detached above a homogeneous incompetent unit. The model folds possess straight fold limbs, a flat crest that parallels both the detachment and the undeformed rocks outside the fold proper, and four straight axial surfaces that define the kink-like geometry of the fold (Fig. 1). Shortening is homogeneously distributed throughout each model and penetrative layer-parallel strain is assumed to be negligible in the competent unit, thereby preserving bed length during fold development for all four models. Because bed length of the competent unit is conserved and because material is not allowed to move in or out of the plane of the cross section, the cross-sectional area of the competent unit is preserved in all models. Constant bed length within the competent unit, while a characteristic of the models and natural detachment folds described by Poblet and McClay (1996), may be an oversimplification for natural detachment folds that experience significant layer-parallel shortening and/or extension (Groshong and Epard, 1994; Epard and Groshong, 1995). However, incorporation of these complexities is beyond the scope of this paper and the current version of DETACH.

Fundamental characteristics of the models are highlighted in Table 1. Model 1, described conceptually by Mitchell and Woodward (1988), assumes that the fold kinematics are controlled by hinge migration. These folds evolve with constant limb dips and accommodate increased shortening by material moving through the axial surfaces and lengthening the fold limbs (Fig. 2A). In contrast, Model 2, which was originally described by De Sitter (1956), is governed by limb rotation. In this case, the limb lengths are determined at the onset of deformation and with increased shortening, the limbs rotate from gentle to steeper dips (Fig. 2B). Dahlstrom (1990) proposed Model 3, where limb lengths grow and limb dips increase with increased shortening (Fig. 2C). Model 4 by Blay et al. (1977) evolves similarly (Fig. 2D), but assumes that the detachment level lies at the depth

Table 1
Fundamental characteristics of detachment fold models in DETACH spreadsheet. All model folds are centered on detachment tip

	Model 1 Mitchell and Woodward (1988)	Model 2 De Sitter (1956)	Model 3 Dahlstrom (1990)	Model 4 Blay et al. (1977)
Fold kinematics	Hinge migration	Limb rotation	Hinge migration & limb rotation	Hinge migration & limb rotation
Area balanced incompetent unit	Yes	Yes	Yes	No
Limb lengths	Variable; ll↑ as s↑	Constant	Variable; ll↑ as s↑	Variable; ll↑ as s↑
Limb dips	Constant	Variable; ld↑ as s↑	Variable; ld↑ as s↑	Variable; ld↑ as s↑
Detachment depth[a]	• z↑ as s↑ • z↓ as ld↑ • z↑ as difference between forelimb/backlimb ld↑	• first z↓, then z↑ as s↑ • z↓ as ll↑	Constant	Constant

Abbreviated text and symbols should be read by replacing each abbreviation or symbol as follows: z = detachment depth, s = slip, ll = limb length, and ld = limb dip. Arrows indicate increasing (↑) and decreasing (↓).
[a]Assumes all other geometric variables are held constant.

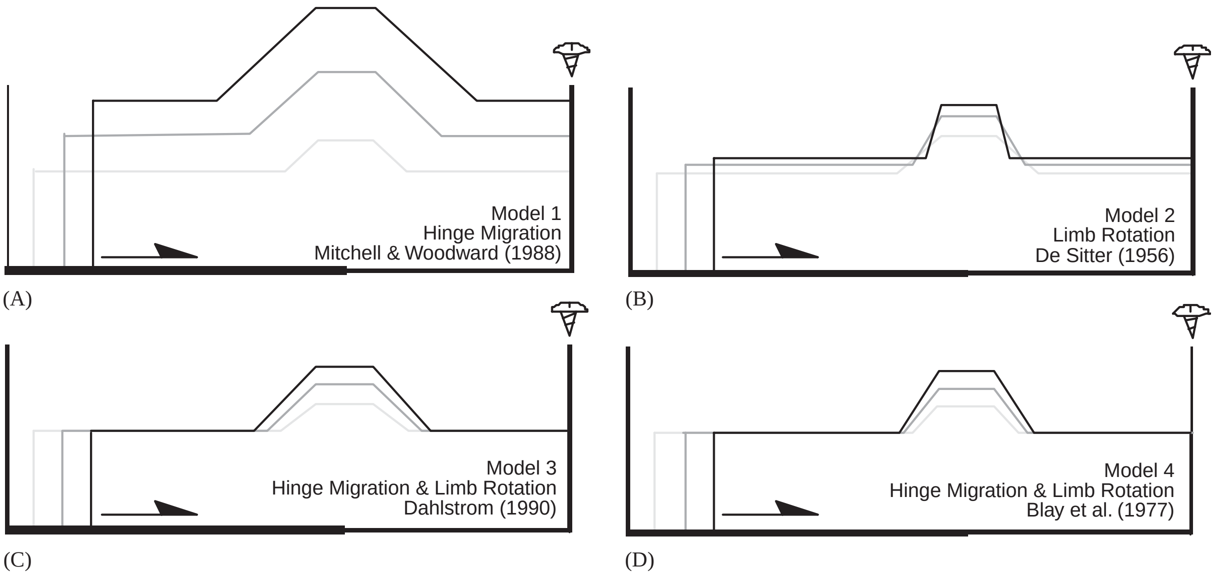

Fig. 2. Detachment fold kinematic models (A) hinge migration model (Mitchell and Woodward, 1988), (B) limb rotation model (De Sitter, 1956), (C) hinge migration and limb rotation (Dahlstrom, 1990), and (D) hinge migration and limb rotation (Blay et al., 1977). Layer represents interface between competent (above) and incompetent units (below). All model folds are centered on detachment tip. Shortening of 5% (light gray), 10% (medium gray), and 15% (black) illustrate kinematic development of each model (note that Model 2 would show a slight initial decrease in detachment depth with increased displacement for shortening values of <5%).

where the two synclinal axial surfaces on either side of the fold meet, rather than basing the fold geometry on the law of conservation of area for both the competent and the incompetent units as does Model 3.

The only difference between our model results and those published by Poblet and McClay (1996) is that by automating the construction of the fold geometries (versus drawing them by hand), we discovered that Poblet and McClay's (1996) Fig. 3 was incorrect with respect to Model 1. The problem exists because Model 1 cannot maintain both a constant limb dip and a constant detachment depth with increasing slip (a characteristic of this model that was also previously noted by Homza and Wallace, 1995). If the limb dip is

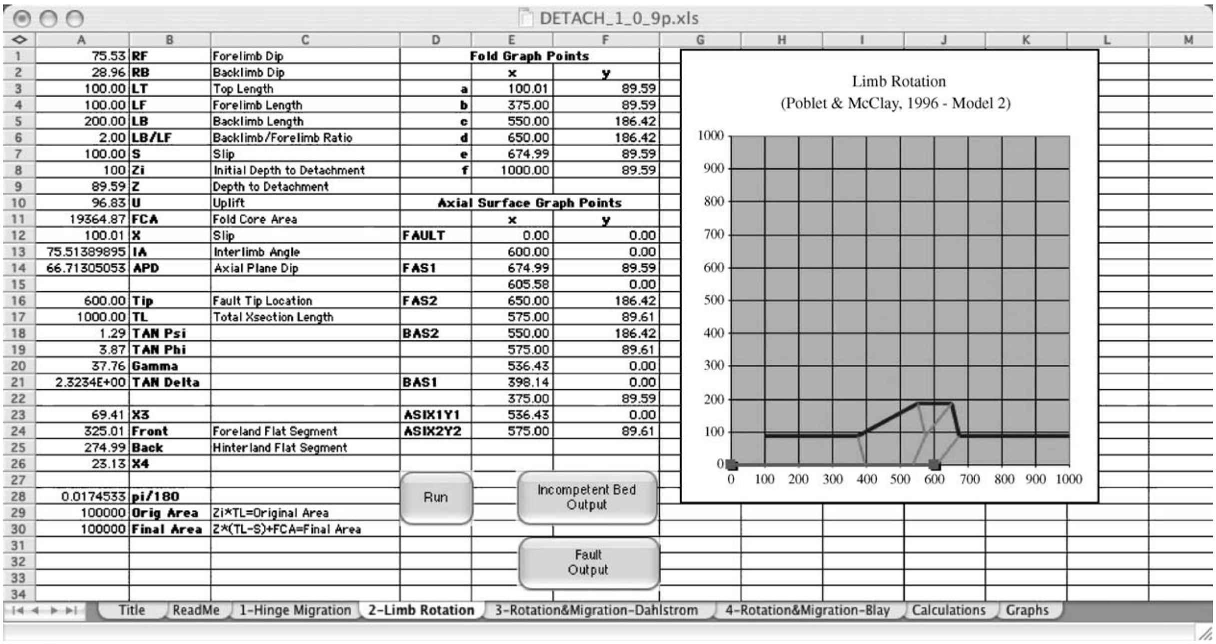

Fig. 3. DETACH program workbook. Each of four models is located on a separate tab of workbook. A model run is started by clicking ‘‘Run’’ button; spreadsheet cells store program input/output and perform additional calculations for plot, graphical output is plotted as a standard Excel™ chart, and data points can be exported by clicking one of ‘‘Output’’ buttons. Additional tabs contain a title page, a ‘‘readme’’ instruction page, a page containing key input/output parameters for all of models, and a composite graphical plot page for all of models.

maintained and cross-sectional area is constant, the detachment depth must vary with increasing slip (Fig. 2A; Table 1).

3. Program description

3.1. Development environment

We used Microsoft Excel™ as our development environment because (1) the program is readily available for both Macintosh and Windows operating systems and is widely used as part of the Microsoft Office™ suite of applications, (2) the Visual Basic for Applications (VBA) component of the Excel™ program can be used to perform the numerical computations necessary to create the models and to generate the dialog-based user interface using standard BASIC programming commands and syntax, and (3) normal spreadsheet features (e.g., cells, charts, etc.) can be used to present the results of the calculations.

3.2. Program overview

We began developing DETACH using a core of BASIC code written by coauthor Josep Poblet, which only performed select calculations for the models. We subsequently added additional calculations, developed a dialog-based user interface, created import/export links between the program and spreadsheet cells, and constructed charts to show the graphical output of the calculations. Each model was placed on a separate tabbed spreadsheet within the Excel™ workbook, with additional tabbed spreadsheets provided to allow comparison of variable quantities and graphs for each model (Fig. 3). The majority of the calculations are performed within the VBA environment, which can be accessed using the VBA macro editor. Relevant calculated variables are transferred to spreadsheet cells for visual analysis, and subsequently, additional calculations are performed by formulas within the cells.

The graphical output is presented in standard Excel™ charts, which have been drawn to a user-specified length and which are formatted to be approximately 1:1 (Fig. 3). In folds formed according to models within DETACH, the cross-sectional length influences the area of the incompetent unit to be considered, and therefore, may affect the final detachment depth (see Fig. 1 in Bulnes and Poblet, 1998 and discussion in Wallace and Homza, 1998). DETACH also allows the user to specify the length of a horizontal crestal panel at the top of the detachment fold (Lt in Fig. 1). The program assumes that the crestal panel maintains constant length during fold development. To model folds that experience length changes of the crestal panel with progressive shortening (for example, to study how crestal length changes affect fold core area (see Figs. 17c and 18c in Bulnes and Poblet, 1999) and/or fold kinematics), the user must create incremental models manually for each stage of fold development. Models are pinned on the foreland edge of the cross section (right side of sections in Fig. 2) and the user determines the exact location of the detachment fold within the cross section by specifying the location of the tip of the fault that underlies the incompetent unit. The default setting for DETACH is for the anticlinal crest to be centered on the fault tip, although this may be changed by editing the appropriate formulas in the spreadsheet cells. Because fold placement in the cross section significantly influences fold kinematics during sequential development of the fold, the user should careful consider fold placement when attempting to model natural structures. Four fold axial surfaces also are drawn in each cross section to better illustrate the overall fold geometry.

3.3. Program workflow

To run the program, the user selects the appropriate tab for the model of interest (Fig. 3). Clicking the "Run" button starts the program and allows the user to set various parameters for the model calculations. These parameters vary depending on the model; the default settings for each dialog are based on values used during the previous model run (and are imported from the appropriate spreadsheet cell). Once the necessary data are entered, the program performs the calculations and updates the appropriate spreadsheet cells. This, in turn, triggers an automatic update of the graph, which redraws the scale, the competent-incompetent horizon boundary, the fault, and the axial surfaces. Clicking one of the "Output" buttons transfers the data points describing the bed or fault to a new spreadsheet where they can be exported as a tab-delimited text file.

4. Applications

4.1. Two-dimensional modeling

Detailed geometric and kinematic analyses of natural detachment folds can be facilitated using DETACH. Specifically, if the 2-D detachment fold geometry is well constrained, one might use models created with DETACH to suggest possible kinematic processes that were operative as the structure developed. Conversely, if the 2-D fold geometry is only partially constrained by field, seismic, and/or well data, one might use DETACH to help interpret possible ranges for the unconstrained parameters (e.g., detachment depth). In addition, DETACH provides a means of modeling possible fold geometries for a given type of fold kinematics. That is, if one can independently ascertain the fold kinematics operative in an area of a known stratigraphic sequence, DETACH can simulate possible geometries for detachment folds that might form.

We chose a well constrained, outcrop-scale example of a natural detachment fold to demonstrate DETACH's modeling capabilities (Fig. 4). The natural detachment fold is located near the crest of the San Rafael Swell in Utah and lies within the Triassic Moenkopi Formation, which is comprised of interbedded siltstones and sandstones. The fold is actually quite small (approximately 3.5 m $\times$ 3.5 m), and the exposure is slightly concave towards the viewer, creating a slight distortion of the fold geometry. We did not correct for this distortion in the following analysis.

We first inserted a photo of the fold into the DETACH chart plot area for the hinge migration (Model 1) and limb rotation (Model 2) models. The bottom of the photo was cropped at the detachment and the chart scaled so that the photo and model exactly coincided (Fig. 4). We then iteratively adjusted the variables for each model until we had the best geometric fit to the natural fold. Of the two models, the limb rotation model (Model 2) provided the overall best geometric match (Fig. 4). The model layer in Fig. 4 illustrates the boundary between the more incompetent siltstones/shales below and the more competent sandstones above. This layer also separates regions of disharmonic folding (e.g., in the fold core) with curved axial surfaces from areas of more parallel folding with straight axial surfaces (Fig. 4).

Because the fold is so well exposed, the benefit of using DETACH was in constraining parameters not measurable in the field. Specifically, our model interpretation would suggest that the fold kinematics are most consistent with development primarily by limb rotation due to approximately 19 cm of slip (easily accounted for by flexural slip as the San Rafael Swell monocline formed). This task could have been done by hand, but the iterative construction and evaluation of model cross sections would have been much more tedious and time-consuming.

4.2. Three-dimensional modeling

DETACH models also can be used to create pseudo-three-dimensional models of detachment folds (cf. Wilkerson et al., 1991). Such pseudo-3-D models can be constructed by linking several serial cross sections in which one or more of the controlling parameters (e.g., displacement, detachment depth) are systematically varied, thereby simulating an along-strike change of that variable. We chose to focus on modeling detachment fold terminations because these portions of the

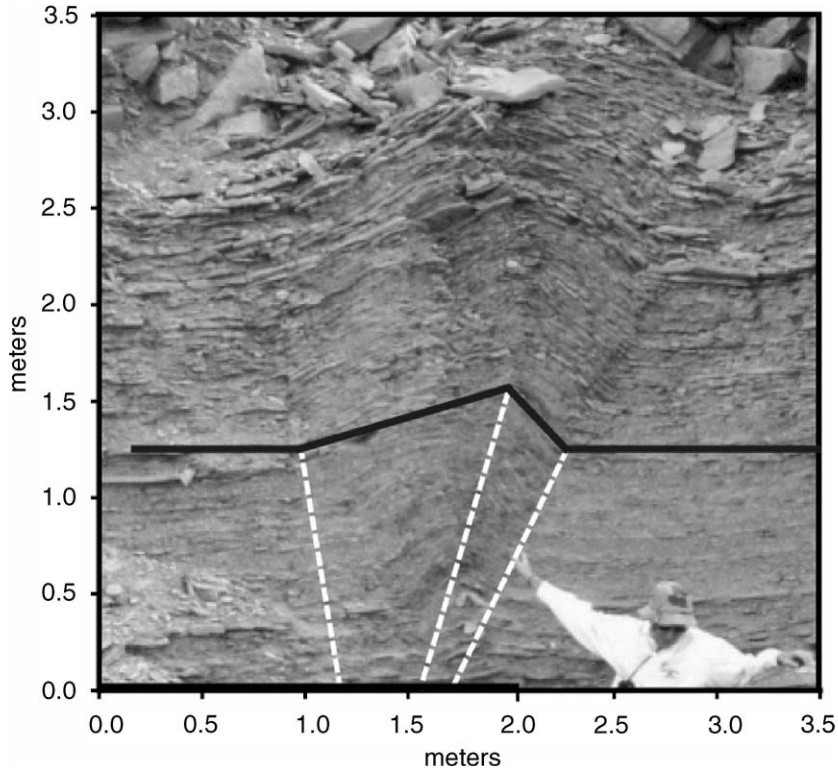

Fig. 4. Two-dimensional model of a natural detachment fold exposed within Triassic Moenkopi Formation near crest of San Rafael Swell in Utah along I-70. Fold geometry is slightly distorted because exposure is slightly concave to viewer. Limb rotation model (Model 2) produces best fit, whereas hinge migration model (Model 1) could not accurately model both limb lengths and positions of axial surfaces.

structure tend to experience the most rapid geometrical changes along strike. The advantage of this approach is that pseudo-three-dimensional models of detachment fold terminations allow one to better (1) understand the lateral evolution of natural detachment folds by looking for similar characteristics/trends between the model and natural detachment fold terminations, (2) constrain the along-strike changes in fold and detachment geometry (e.g., changes in detachment depth) of natural detachment folds in areas where these features are not well constrained, and (3) differentiate between the various geometric and kinematic models by comparing them in the third dimension.

We used DETACH to construct pseudo-three-dimensional models of detachment fold terminations using Poblet and McClay's (1996) geometric and kinematic models. We chose to construct detachment fold terminations produced solely by a loss of displacement along the length of the fold, effectively creating a linear along-strike displacement gradient that could be represented by an angle (e.g., Wilkerson et al., 1991; Wilkerson, 1992), although one could investigate any number of along-strike changes (e.g., variations in detachment depth, limb dip, limb length, etc.). We focused our study exclusively on the pure hinge migration (Model 1) and limb rotation (Model 2) models because they represent kinematic end members of the range of models described by Poblet and McClay (1996).

The general procedure that we used was to create the model cross sections in DETACH and then to export the sections into the Geosec2D™ cross section construction/modeling program, where additional folded layers were created by projecting upward from the imported horizon from DETACH using a constant thickness, dip-domain geometry. In addition, within Geosec2D™ each section was associated with a different map-view section line (giving each *xz*-section a *y*-component), and then was exported into the Gocad™ 3-D modeling program. In Gocad™ 3-D surfaces were constructed by linking corresponding horizons on adjacent serial sections (Fig. 5). Finished models were subsequently sliced along the *z*-axis with Gocad™ to simulate erosion in order to more easily compare the map-view expression of the various models (Fig. 5).

Using DETACH, we constructed serial cross sections for both Models 1 and 2 by varying along-strike shortening to simulate a 10° displacement gradient. Because the governing equations are different for the

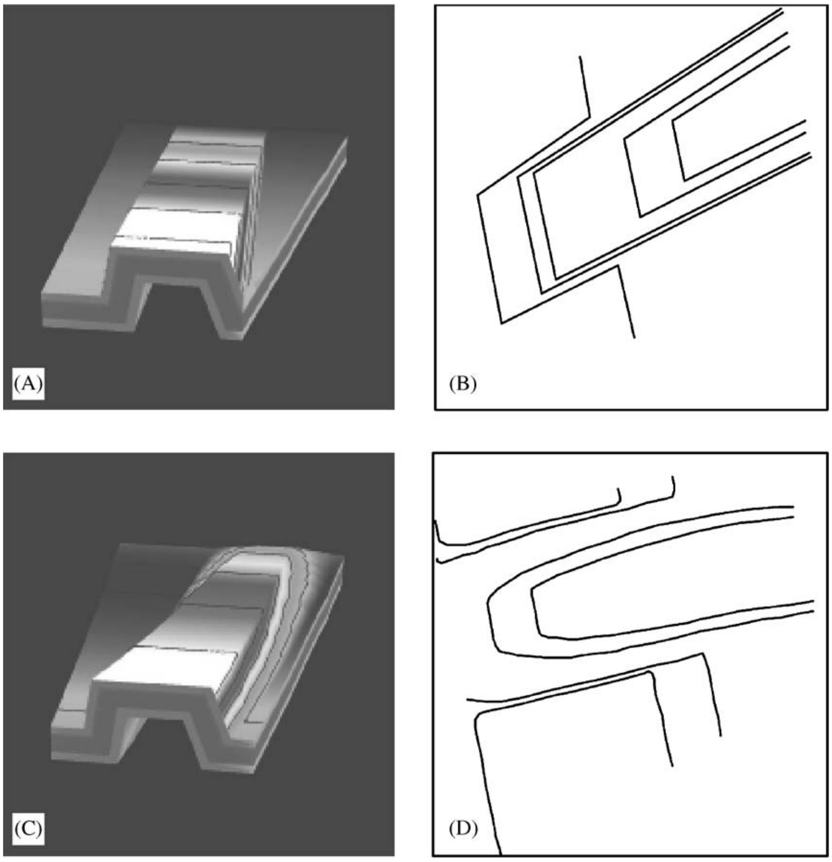

Fig. 5. Pseudo-three-dimensional models and synthetic geologic maps of detachment fold terminations. (A) 3-D model of a Model 1 (hinge migration) detachment fold termination with a 10° lateral displacement gradient; (B) geologic map sliced through model shown in part (A); (C) 3-D model of a Model 2 (limb rotation) detachment fold termination with a 10° lateral displacement gradient; (D) geologic map sliced through model shown in part (C). On 3-D models, displacement is from left to right with greatest displacement on side nearest viewer; whereas on geologic maps, displacement is from bottom to top with greatest displacement on right side of map.

two models, we could not keep the same variables constant in both models. For Model 1, limb dips were set to 70° for the backlimb and 80° for the forelimb; limb lengths, however, systematically increased along-strike as displacement increased (Fig. 5). In contrast, for Model 2, limb lengths were set to 2362.5 units for the backlimb and 2250 units for the forelimb; limb dips, however, increased as displacement increased along strike (Fig. 5). All of the other settings were the same for both models. These values were chosen so that cross sections with the largest displacement for each model were similar (Fig. 5A and C).

Fig. 5 illustrates a comparison of the two models assuming a horizontal detachment that is at a constant stratigraphic level. Model 1 (hinge migration; Fig. 5A and B) possesses straight axial surfaces in map view with tilted layers in areas outside the plunging anticline. These dips reflect the larger detachment depth (i.e., thickening of the incompetent unit) produced by increasing the slip. Model 2 (limb rotation; Fig. 5C and D) exhibits curved axial surfaces in map view due primarily to the along-strike increase in limb dip with increasing displacement. The regions outside the plunging anticline possess a subsidiary syncline whose axis is nearly perpendicular to the main fold axis. This secondary fold reflects the initial shallowing and subsequent increase in the detachment depth (resulting from thickness changes of the incompetent unit) produced by Model 2 in areas of low displacements. Comparison of the two models suggests that significant differences exist that might allow geologists to better constrain the geometries and kinematics of natural detachment folds as well as to infer the relative significance of variables that control 3-D detachment fold geometry.

5. Discussion

The DETACH Excel™ spreadsheet provides a reliable, simple, and rapid means for generating cross sections of detachment folds using the four models described by Poblet and McClay (1996). Using this program to compare model results with natural structures might help (1) shed insight on possible kinematic processes that were operative as the natural structures developed and/or (2) reduce the range of possible values for poorly constrained fold parameters (e.g., shortening, detachment depth, etc.). While DETACH accurately portrays the finite geometries and kinematics as prescribed by the original models, interpretations of the sequential development of detachment folds are also influenced by user input (e.g., crestal length variations, fold placement within the cross section, etc.). Therefore, as with using any model to simulate natural phenomena, it is important for users to understand the implications of their decisions during model construction to ensure that implausible scenarios are not contrived during the modeling process.

Acknowledgements

The authors wish to thank Richard H. Groshong, Jr. and Wesley K. Wallace for their careful and insightful reviews. The authors are indebted to Paradigm Geophysical, Inc. for the use and support of the Geosec2D^{TM} structural modeling software, and to Earth Decision Sciences for the use of the Gocad^{TM} 3-D modeling software. Support for this work was provided by NSF grant EAR-9972993 to Fischer and G. Perry (and by an NSF-ROA supplement to this grant to Wilkerson). The Science Research Fellows and the Faculty Development Programs at DePauw University also supported Wilkerson and Wilson. Poblet acknowledges support by projects MCT-01-REN1734-C03-02/MAR, BTE2002-00187, BTE2002-04316-C03-03 and BTE2001-5365-E funded by the Spanish Ministry of Science and Technology.

References

Apotria, T.G., Wilkerson, M.S., 2002. Seismic expression and kinematics of a fault-related fold termination: Rosario Structure, Maracaibo Basin, Venezuela. Journal of Structural Geology 24 (4), 671–689.

Atkinson, P.K., Wallace, W.K., 2003. Competent unit thickness variation in detachment folds in the northeastern Brooks Range, Alaska: geometric analysis and a conceptual model. Journal of Structural Geology 25 (10), 1751–1771.

Blay, P.K., Cosgrove, J.W., Summers, J.M., 1977. An experimental investigation of the development of structures in multi-layers under the influence of gravity. Journal of the Geological Society of London 133 (4), 329–342.

Bulnes, M., Poblet, J., 1998. Detachment folds with fixed hinge and variable detachment depth, northeastern Brooks Range, Alaska. Journal of Structural Geology 20 (11), 1587–1590.

Bulnes, M., Poblet, J., 1999. Estimating the detachment depth in cross sections involving detachment folds. Geological Magazine 136 (4), 395–412.

Chamberlin, R.T., 1910. The Appalachian folds of central Pennsylvania. Journal of Geology 18, 228–251.

Dahlstrom, C.D.A., 1970. Structural geology in the eastern margin of the Canadian Rocky Mountains. Bulletin of Canadian Petroleum Geology 18 (3), 332–406.

Dahlstrom, C.D.A., 1990. Geometric constraints derived from the law of conservation of volume and applied to evolutionary models for detachment folding. American Association of Petroleum Geologists Bulletin 74 (3), 336–344.

De Sitter, L.U., 1956. Structural Geology, first ed. McGraw-Hill Book Co., New York 552pp.

Epard, J.-L., Groshong, R.H., 1993. Excess area and depth to detachment. American Association of Petroleum Geologists Bulletin 77 (8), 1291–1302.

Epard, J.-L., Groshong, R.H., 1995. Kinematic model of detachment folding including limb rotation, fixed hinges, and layer-parallel strain. Tectonophysics 247 (1–4), 85–103.

Groshong, R.H., Epard, J.-L., 1994. The role of strain in area-constant detachment folding. Journal of Structural Geology 16 (5), 613–618.

Hardy, S., Poblet, J., 1994. Geometric and numerical model of progressive limb rotation in detachment folds. Geology 22 (4), 371–374.

Homza, T.X., Wallace, W.K., 1995. Geometric and kinematic models for detachment folds with fixed and variable detachment depths. Journal of Structural Geology 17 (4), 575–588.

Homza, T.X., Wallace, W.K., 1997. Detachment folds with fixed hinges and variable detachment depth, northeastern Brooks Range, Alaska. Journal of Structural Geology 19 (3–4), 337–354.

Jamison, W.R., 1987. Geometric analysis of fold development in overthrust terranes. Journal of Structural Geology 9 (2), 207–219.

Mitchell, M.M., Woodward, N.B., 1988. Kink detachment fold in the southwest Montana fold and thrust belt. Geology 16 (2), 162–165.

Mitra, S., 1990. Fault-propagation folds: geometry, kinematics, and hydrocarbon traps. American Association of Petroleum Geologists Bulletin 74 (6), 921–945.

Mitra, S., 1992. Balanced structural interpretations in fold and thrust belts. In: Mitra, S., Fischer, G.W. (Eds.), Structural Geology of Fold and Thrust Belts. John Hopkins University Press, Baltimore, MD, pp. 53–77.

Poblet, J., Hardy, S., 1995. Reverse modeling of detachment folds: application to the Pico de Aguila anticline in the South Central Pyrenees (Spain). Journal of Structural Geology 17 (12), 1707–1724.

Poblet, J., McClay, K.R., 1996. Geometry and kinematics of single-layer detachment folds. American Association of Petroleum Geologists Bulletin 80 (7), 1085–1109.

Suppe, J., 1983. Geometry and kinematics of fault-bend folding. American Journal of Science 283 (9), 684–721.

Suppe, J., Medwedeff, 1990. Geometry and kinematics of fault-propagation folding. Eclogae Geologicae Helvetica 83 (3), 409–454.

Wallace, W.K., Homza, T.X., 1998. Detachment folds with fixed hinges and variable detachment depth, northeastern Brooks Range, Alaska. Reply. Journal of Structural Geology 20 (11), 1591–1595.

Wilkerson, M.S., 1992. Differential transport and continuity of thrust sheets. Journal of Structural Geology 14 (6), 749–751.

Wilkerson, M.S., Medwedeff, D.A., Marshak, S., 1991. Geometrical modeling of fault-related folds: a pseudo-three-dimensional approach. Journal of Structural Geology 13 (7), 801–812.

Wilkerson, M.S., Wellman, P.C., 1993. Three-dimensional geometry and kinematics of the Gale-Buckeye thrust system, Ouachita fold-thrust belt, Latimer & Pittsburg Counties, Oklahoma. American Association of Petroleum Geologists Bulletin 77 (6), 1082–1100.